SCIENCE CHINA
Physics, Mechanics & Astronomy

• Article •

April 2020 Vol. 63 No. 4: 244711
https://doi.org/10.1007/s11433-019-1458-4

Non-premixed turbulent combustion modeling based on the filtered turbulent flamelet equation

Jian Zhang[1], LiPo Wang[2*], and YuQing Guo[2]

[1] *State Key Laboratory of Nonlinear Mechanics (LNM), Chinese Academy of Sciences, Beijing 100190, China;*
[2] *UM-SJTU Joint Institute, Shanghai Jiao Tong University, Shanghai 200240, China*

Received September 2, 2019; accepted October 10, 2019; published online November 25, 2019

In turbulent combustion simulations, the flow structure at the unresolved scale level needs to be reasonably modeled. Following the idea of turbulent flamelet equation for the non-premixed flame case, which was derived based on the filtered governing equations (L. Wang, Combust. Flame **175**, 259 (2017)), the scalar dissipation term for tabulation can be directly computed from the resolved flowing quantities, instead of solving species transport equations. Therefore, the challenging source term closure for the scalar dissipation or any assumed probability density functions can be avoided; meanwhile the chemical sources are closed by scaling relations. The general principles are discussed in the context of large eddy simulation with case validation. The new model predictions of the bluff-body flame show sufficiently improved results, compared with these from the classic progress-variable approach.

turbulent combustion modeling, turbulent flamelet equation, large eddy simulation, non-premixed flame

PACS number(s): 47.27.E-, 47.70.Pq, 02.70.-c

Citation: J. Zhang, L. P. Wang, and Y. Q. Guo, Non-premixed turbulent combustion modeling based on the filtered turbulent flamelet equation, Sci. China-Phys. Mech. Astron. **63**, 244711 (2020), https://doi.org/10.1007/s11433-019-1458-4

1 Introduction

In reactive turbulence, both the spatial and temporal scales are involved and the fine structures need to be modeled at the affordable mesh level. From the fundamental modeling point of view, large-eddy simulation (LES) techniques with different sub-grid models have been demonstrated the superiority to Reynolds-averaged Navier-Stokes (RANS) approaches, especially in predicting the turbulent mixing process. For the non-premixed turbulent combustion simulations, scalar dissipation and scalar variance are critical modeling parameters, for instance in mixture fraction-based models, including flamelet models [1, 2] and the conditional moment closure [3]. In the transported probability density function approaches the scalar dissipation and scalar variance are also needed [4] to obtain variables such as mixing coefficients [5]. In the classical steady laminar flamelet model, the averaged mixture fraction and scalar dissipation rate [1, 2] with prescribed probability density functions (PDFs) function as the entries of a generated chemistry table, from which quantities and species are retrieved. However, the scalar variance and scalar dissipation rate are the main parameters to be modeled with unavoidable model uncertainties [6-13].

The applications and possible improvements of flamelet models have been the research topics of interest [1, 2, 14, 15], because of the advantage in computational cost reduction by mapping the dependent quantities to a low-dimensional parametric space, and at the same time without loss of accuracy

*Corresponding author (email: Lipo.Wang@sjtu.edu.cn)

via the solution of the laminar flamelet equation. Especially in the context of LES, the progress variable approach adopts the filtered progress variable, which is a quantity that can be directly solved [2], as one of the chemistry table entries. Thus the model uncertainty can be reduced with improved performance [15-19], compared with other flamelet models. However, in the progress variable approach it still remains as an issue to model the filtered scalar variance.

To develop new modeling ideas, an interesting effort is to understand directly the filtered flame statistics. Wang [20] derived a so-called filtered turbulent flamelet equation in studying the structure of the filtered non-premixed turbulent flame. Because the normal of filtered turbulent flame fronts can well preserve the alignment relations with the species gradients, the filtered turbulent flamelet equation can be reasonably simplified, where the filtered species mass fractions are the functions of filtered mixture fraction and a named turbulent scalar dissipation rate can be directly calculated without any prescribed PDF and the model of scalar variance. The present work aims to develop a new modeling idea based on the analysis of the turbulent flamelet equation, with the numerical validation of the Sydney bluff-body flame.

2 Formulation and analysis

In non-premixed combustion, the governing equations of mass, species and mixture fraction Z are

$$\frac{\partial \rho}{\partial t} + \nabla \cdot (\rho \mathbf{u}) = 0, \tag{1}$$

$$\frac{\partial \rho \phi_k}{\partial t} + \nabla \cdot (\rho \mathbf{u} \phi_k) = -\nabla \cdot (\rho \alpha_k \nabla \phi_k) + \rho \omega_k, \tag{2}$$

$$\frac{\partial \rho Z}{\partial t} + \nabla \cdot (\rho \mathbf{u} Z) = \nabla \cdot (\rho D \nabla Z), \tag{3}$$

respectively. Here ρ is the fluid density, $\mathbf{u}$ is the flow velocity, α_k and $\phi_k, (k = 1, \ldots, n)$ are diffusion coefficient and the mass fraction of species k in a mixture of n different species, respectively.

After the filtering operation in LES at the resolved scale, together with the gradient transport models as:

$$\bar{\rho}(\widetilde{\mathbf{u}Z} - \widetilde{\mathbf{u}}\widetilde{Z}) = \bar{\rho} D_{\mathrm{T}} \nabla \widetilde{Z}, \tag{4}$$

$$\bar{\rho}(\widetilde{\mathbf{u}Y_i} - \widetilde{\mathbf{u}}\widetilde{Y_i}) = \bar{\rho} D_{\mathrm{T},i} \nabla \widetilde{Y_i}, \tag{5}$$

it yields

$$\frac{\partial \bar{\rho}\widetilde{Z}}{\partial t} + \nabla \cdot (\bar{\rho}\widetilde{Z}\widetilde{\mathbf{u}}) = \nabla \cdot [\bar{\rho}(D + D_{\mathrm{T}}) \nabla \widetilde{Z}] = \nabla \cdot [\bar{\rho} \mathfrak{D}_{\mathrm{T}} \nabla \widetilde{Z}], \tag{6}$$

for the filtered mixture fraction equation $\widetilde{Z}$, and

$$\frac{\partial \bar{\rho}\widetilde{Y_i}}{\partial t} + \nabla \cdot (\bar{\rho}\widetilde{Y_i}\widetilde{\mathbf{u}}) = \nabla \cdot [\bar{\rho}(D_i + D_{\mathrm{T},i}) \nabla \widetilde{Y_i}] + \overline{\omega_i}$$
$$= \nabla \cdot [\bar{\rho} \mathfrak{D}_{\mathrm{T},i} \nabla \widetilde{Y_i}] + \overline{\omega_i} \tag{7}$$

for the filtered species concentration $\widetilde{Y_i}$. Here $\bar{\cdot}$ and $\widetilde{\cdot}$ denote the filtered and density-weighted filtered quantities, respectively.

Following the derivation in ref. [20], we can introduce a Lagrangian coordinate system to map to the mixture fraction Z space as:

$$(x_1, x_2, x_3, t) \mapsto (Z, Z_2, Z_3, \tau), \tag{8}$$

where $\tau = t$ and Z_2 and Z_3 are two auxiliary coordinates, which are locally tangential to the $\widetilde{Z}$ isosurface and dependent on both x_i and t. To simplify the following mathematic expression, Z_2 and Z_3 are chosen as the curvilinear coordinates on the Z isosurfaces and orthogonal to each other. For more detailed discussion the reader can be referred to the analysis by ref. [21]. Thus the gradient operator ∇ can be expressed as:

$$\nabla = \mathbf{n}\frac{\partial \widetilde{Z}}{\partial \mathbf{n}}\frac{\partial}{\partial \widetilde{Z}} + \frac{\mathbf{t}_2}{h_2}\frac{\partial}{\partial Z_2} + \frac{\mathbf{t}_3}{h_3}\frac{\partial}{\partial Z_3} = \mathbf{n}\frac{\partial \widetilde{Z}}{\partial \mathbf{n}}\frac{\partial}{\partial \widetilde{Z}} + \nabla_{\perp}, \tag{9}$$

where $\mathbf{n}$ is the unit normal to the $\widetilde{Z}$ isosurface, $\mathbf{t}_2$ and $\mathbf{t}_3$ are the unit directional vector for the Z_2 and Z_3 coordinates, and h_2 and h_3 are their corresponding Lamé coefficients, and $\nabla_{\perp}$ denotes the gradient operator in the surface spanned by Z_2 and Z_3. Based on these, Wang [20] further derived the turbulent flamelet equation as follows:

$$\begin{aligned}\bar{\rho}\frac{\partial \widetilde{Y_i}}{\partial \tau} + \bar{\rho}\Big(\widetilde{\mathbf{u}} \cdot \nabla_{\perp}\widetilde{Y_i} + \frac{\partial \widetilde{Y_i}}{\partial Z_2}\frac{\partial Z_2}{\partial t} + \frac{\partial \widetilde{Y_i}}{\partial Z_3}\frac{\partial Z_3}{\partial t}\Big)& \\ = \frac{1}{2Le_{\mathrm{T}}}\bar{\rho}\chi\frac{\partial^2 \widetilde{Y_i}}{\partial \widetilde{Z}^2} + \frac{\partial \widetilde{Y_i}}{\partial \widetilde{Z}}\nabla \cdot \Big[\bar{\rho}(\mathfrak{D}_{\mathrm{T},i} - \mathfrak{D}_{\mathrm{T}})\mathbf{n}\frac{\partial \widetilde{Z}}{\partial n}\Big]& \\ + \nabla \cdot (\bar{\rho}\mathfrak{D}_{\mathrm{T},i}\nabla_{\perp}\widetilde{Y_i}) + \overline{\omega_i},&\end{aligned} \tag{10}$$

where the turbulent scalar dissipation χ is defined as:

$$\chi = 2D_{\mathrm{T}}\Big(\frac{\partial \tilde{Z}}{\partial n}\Big)^2$$

and the turbulent scalar dissipation Lewis number $Le_{\mathrm{T}} = D_{\mathrm{T}}/\mathfrak{D}_{\mathrm{T},i}$. Here $\nabla_{\perp}$ denotes the gradient operator in the surface spanned by Z_2 and Z_3. D_{T} and $D_{\mathrm{T},i}$ can be calculated by orientational average of the flow field information as $D_{\mathrm{T}} = (\tilde{\mathbf{u}}\tilde{Z} - \widetilde{\mathbf{u}}\widetilde{Z}) \cdot \nabla \tilde{Z} / \left|\nabla \tilde{Z}\right|^2$ and $D_{\mathrm{T},i} = (\tilde{\mathbf{u}}\tilde{Y}_i - \widetilde{\mathbf{u}}\widetilde{Y_i}) \cdot \nabla \tilde{Y}_i / \left|\nabla \tilde{Y}_i\right|^2$.

For the filtered turbulent flame fronts, because of the alignment relations among the gradients of the species and mixture fraction [20], eq. (10) can be reasonably simplified as:

$$\frac{1}{2Le_{\mathrm{T}}}\bar{\rho}\chi\frac{\partial^2 \widetilde{Y_i}}{\partial \widetilde{Z}^2} + \overline{\omega_i(Y_1, Y_2, ..., T)} = 0, \tag{11}$$

by neglecting the time derivative and lateral derivative terms. This equation has the same form as the steady laminar flamelet equation. However, the involved quantities are of

different implications. On the one hand, the turbulent scalar dissipation term χ needs not to be modeled, because both D_{T} and $(\frac{\partial \tilde{Z}}{\partial n})^2$ can be calculated directly; on the other hand, it is still challenging to obtain the non-filtered species values Y_i to calculate the chemical source term $\overline{\omega_i(Y_1, Y_2, ..., T)}$. To attack this difficulty, the scaling relations [20] of the filtered species are revisited. According to ref. [20], in the inertial range, the following scaling relation exists conditional on the stoichiometric Z isosurface:

$$\langle \tilde{Y}_i(\mathbf{r})_{,l} - Y_i(\mathbf{r}) \rangle \sim C_i l^{\alpha_i}, \tag{12}$$

where the two unknown parameters C_i and α_i can be determined if the filtering operation is performed at two different length scale levels, which is widely used in the dynamic subgrid models in LES. Here the average operation $\langle \cdot \rangle$ is defined with respect to the entire flame surface at different $\mathbf{r}$. Physically, such scaling relation is an imprint of the structure similarity at different scales. In principle, once the grid size is fine for LES, such scaling relations will hold. In summary, the turbulent flamelet solution can be obtained by combining eqs. (11) and (12). More details will be noted in the numerical description part.

3 Case validation and numerical results

3.1 Numerical setup

The Sydney bluff-body burner is investigated here to validate the new model. As shown in Figure 1(a) the burner consists of a cylindrical bluff-body with an orifice and is centered in a wind tunnel that supports a co-flowing air stream. Both the fuel and the air jets have the same inlet temperature 300 K. Following the experimental conditions [22], the fuel through the central nozzle is composed of methane and hydrogen (1:1 by volume) with a stoichiometric mixture fraction $Z_{\mathrm{st}} = 0.05$. The bluff-body diameter is $D = D_{\mathrm{b}}$ =50 mm and the fuel jet diameter is D_j = 3.6 mm. The Reynolds number $Re = U_{\mathrm{j}} D_{\mathrm{j}}/\nu = 15800$, where U_{j} represents the bulk velocity of the turbulent fuel jet and ν is the gas kinematic viscosity. U_{j} and the ambient coflow bulk velocity U_{e} are set as 108 and 35 m/s, respectively.

In order to capture effectively the flow and flame characteristics, the numerical mesh is locally refined with total 256 × 165 × 64 grid points in axial, radial and circumferential directions, respectively. As shown in the cross cut Figure 1(b), the refined parts include the region near the inlet, the shear layer surrounding the fuel jet and the edge of bluff body [23, 24]. The finite volume method is used to discrete the governing equations, and the staggered grid improves the

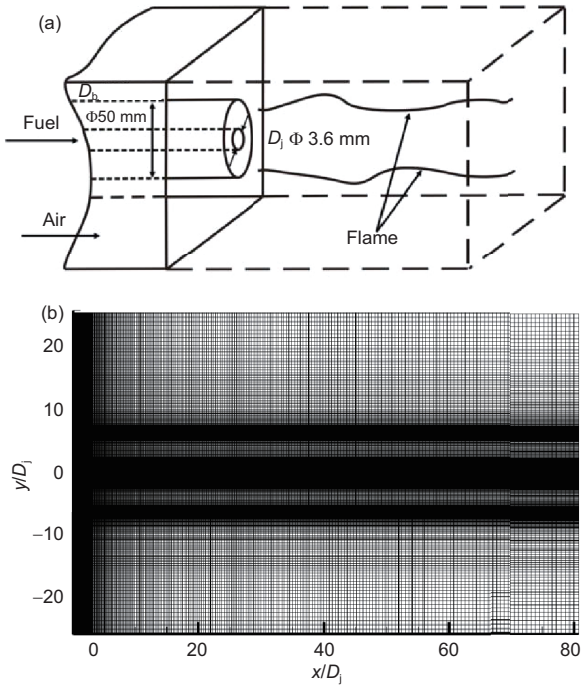

Figure 1 (a) Schematic of the Bluff body burner; (b) cross cut of the numerical mesh.

precision of the difference scheme and the stability of the numerical solution. For the spatial derivatives, both the convection and the diffusion term use the second-order scheme; for the time derivative, the second-order semi-implicit method is adopted. The dynamics subgrid stress model is used in LES.

As a preliminary test, a four-step global mechanism suggested by Jones and Lindstedt [25] is used as the representative combustion chemistry. In the previous studies [25-27], this mechanism has been validated for different non-premixed combustion cases. The scaling relations can be determined by iteration as follows. Starting from an approximate chemical table, for instance the one used for the laminar flamelet case, a tentative flow field is obtained. Through the field filtering at two different scale levels, parameters in eq. (12) can be determined to update the chemical table. The flow field will be recalculated to renew the scaling relation. Typically two iterations are sufficient to ensure a good solution convergence.

3.2 Results and discussion

The simulation results from the present turbulent flamelet method using the JL mechanism (TFM-JL) will be compared with the experimental measurements (Exp.), the flamelet/progress variable approach using the JL mechanism (FPV-JL), and the literature results from other methods as well, including the steady flamelet/progress variable approach using detailed chemical mechanism of GRI-Mech

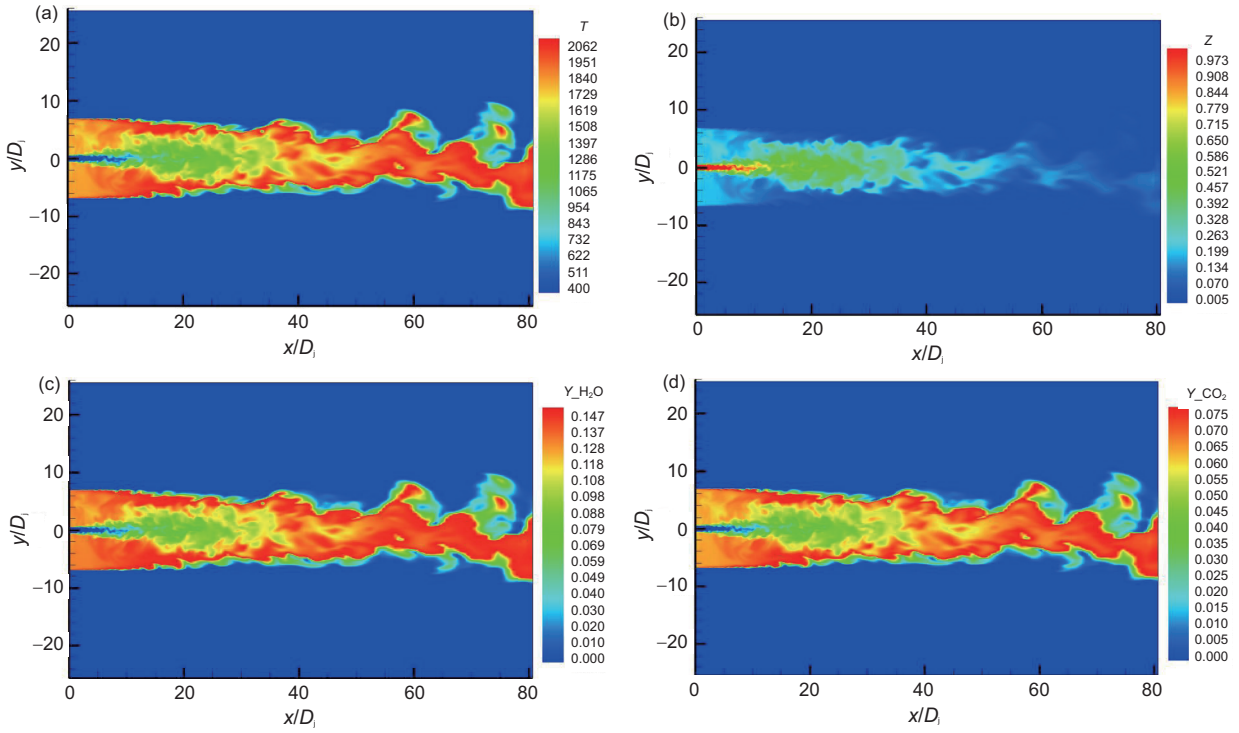

Figure 2 (Color online) Contour plots for (a) temperature, (b) mixture fraction, (c) mass fraction of H_2O and (d) mass fraction of CO_2.

2.11 [24] (FPV-GRIMech) and the steady laminar flamelet model using detailed chemical mechanism with 97 species and 629 chemical reactions (LFM) [23]. In the FPV method, the Favre-averaged scalar is modeled as:

$$\widetilde{\phi} = \widetilde{\phi}(\widetilde{Z}, \widetilde{Z''^2}, \widetilde{C}), \tag{13}$$

where Z''^2 is the the mixture fraction variance and the reaction progress variable C is defined as a linear combination of major species as $C = Y_{CO_2} + Y_{CO} + Y_{H_2O} + Y_{H_2}$. The presumed beta-PDF of the mixture fraction and a Dirac-delta function is used as the conditional PDF of the reaction progress variable.

Figure 2 presents the instantaneous contour plots of representative field quantities, including the temperature, mixture fraction and major species.

The radial distribution of mean velocity component U in Figure 3 is in very good agreement with the experiment data. At downstream, the difference is bit larger, which can be explained by the reduced resolution. The recirculation zone, which is important to stabilize the combustion, is also clearly visualized. Although only the simplified JL mechanism is used, the present model shows satisfactory accuracy, compared with other models with detailed chemistry.

In Figure 4 the satisfactory match of the mixture fraction profile with the experiment data implies that the present model can accurately capture the mixing layer thickness. In the recirculation zone with negative velocity component U, the mixture fraction remains a degree of magnitude higher than the stoichiometric ratio, which means oxygen-enriched combustion in the recirculation zone.

The predicted mean temperature is shown in Figure 5. Compared with the progress-variable approach model, where the laminar flamelet database and assumed PDF are used, the temperature profile from the turbulent flamelet model is closer to the experimental result, especially in predicting the

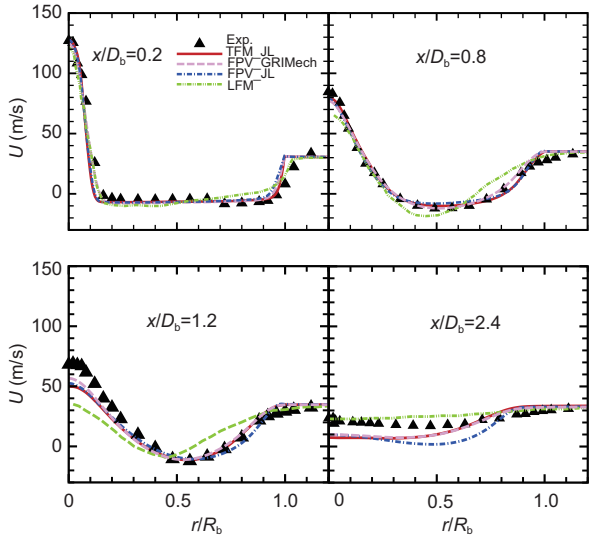

Figure 3 (Color online) The radial distribution of mean axial velocity U profile on different axial positions from the experimental measurements (Exp.), the laminar flamelet/progress variable mode (FPV) and the turbulent flamelet model (TFM).

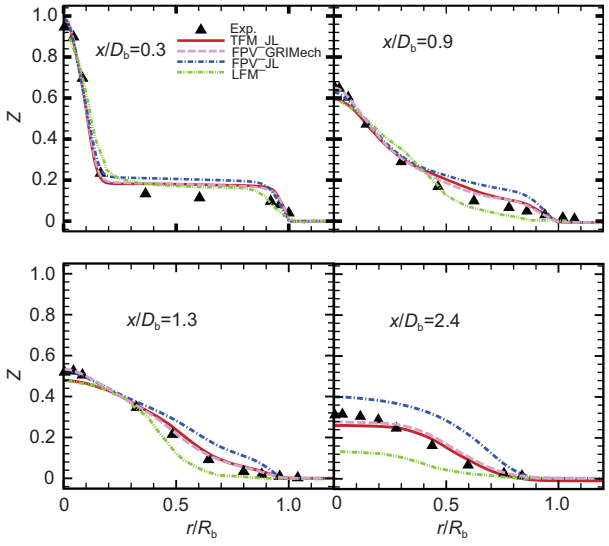

Figure 4 (Color online) Same as Figure 3, but for the mixture fraction Z.

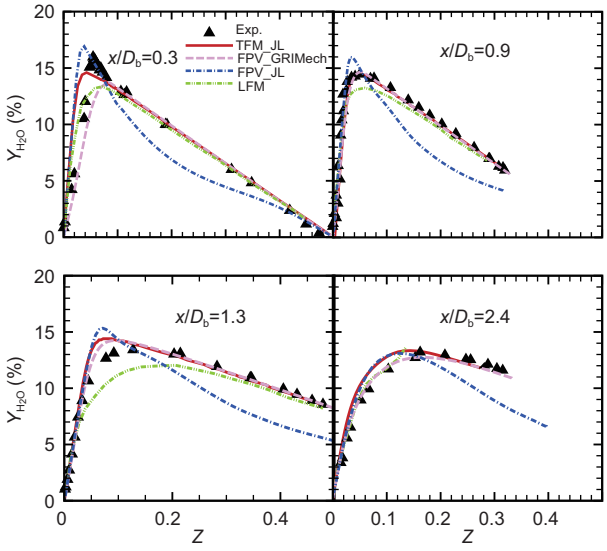

Figure 6 (Color online) Same as Figure 3, but for the species Y_{H_2O}.

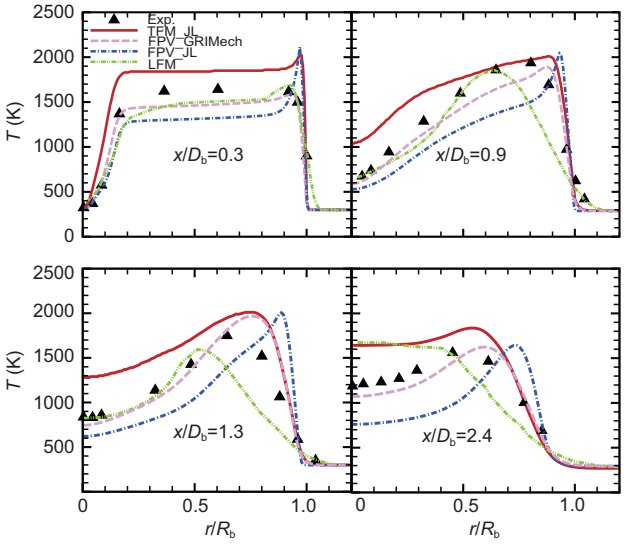

Figure 5 (Color online) Same as Figure 3, but for the mean temperature T.

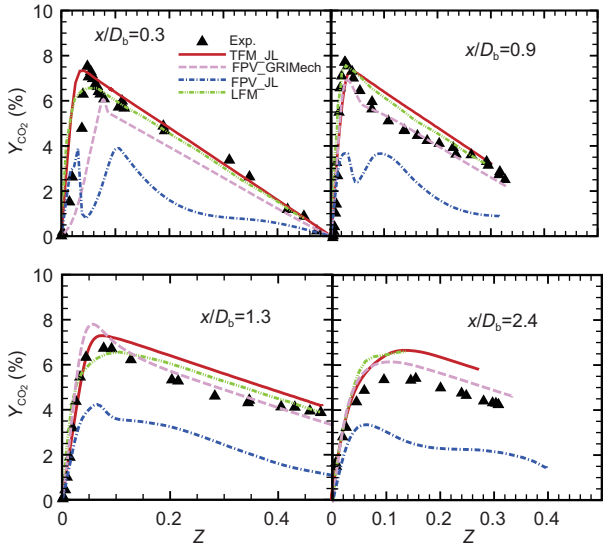

Figure 7 (Color online) Same as Figure 3, but for the species Y_{CO_2}.

peak value. The slight overshot of the temperature can be attributed to the fact that the extinction-reigntion behavior is not sufficiently accounted. Overall, the temperature profile can be well captured.

The predictions of representative species, e.g., H_2O and CO_2, are shown in Figures 6 and 7. The new model results are clearly better, compared with the flamelet/progress variable approach. Here only the four-step simplification mechanism is used. It is reasonable to expect further improvements if a more detailed chemical mechanism is adopted, together with the extinction-reigntion consideration. For more details of the numerical implementation and simulation details, readers can be referred to ref. [28].

4 Conclusions

New modeling idea of non-premixed turbulent combustion is presented based on the analysis of the filtered flame structure [20]. The filtered governing equations in the context of LES have been revisited and a so-called filtered turbulent flamelet eq. (10) can be derived. In contrast to the laminar flamelet equation, the challenging scalar dissipation term in the filtered flamelet equation can be directly calculated, i.e. this quantity can be considered as numerically 'accurate' without modeling or any assumed PDF. Meanwhile, the strongly nonlinear chemical sources are closed using the scaling relations, as suggested by eq. (12). Numerical results

show that compared with the standard progress variable approach, the accuracy of model prediction can be sufficiently improved. In spite of these advantages, there are still remaining challenging issues, for example, the local extinction, self-ignition and reignition need to be accounted for more complex cases.

This work was supported by the National Natural Science Foundation of China (Grant No. 11572330). LiPo Wang thanks the support from the Engineering Research Center of Gas Turbine and Civil Aero Engine, Ministry of Education; Jian Zhang thanks the support from International Clean Energy Talent Program by China Scholarship Council (Grant No. 201904100044) and Open founding of National Key Laboratory of Science and Technology on Aero-Engine Aero-Thermodynamics (Grant No. 6142702180307).

1 N. Peters, *Turbulent Combustion* (Cambridge University Press, Cambridge, 2000), p. 212.
2 C. D. Pierce, and P. Moin, J. Fluid Mech. **504**, 73 (1999).
3 A. Y. Klimenko, and R. W. Bilger, Prog. Energy Combust. Sci. **25**, 595 (1999).
4 S. B. Pope, Prog. Energy Combust. Sci. **11**, 119 (1985).
5 V. Eswaran, and S. B. Pope, Phys. Fluids **31**, 506 (1988).
6 G. Balarac, H. Pitsch, and V. Raman, Phys. Fluids **20**, 035114 (2008).
7 G. Balarac, H. Pitsch, and V. Raman, Phys. Fluids **20**, 091701 (2008).
8 A. W. Cook, and J. J. Riley, Phys. Fluids **6**, 2868 (1994).
9 C. M. Kaul, V. Raman, G. Balarac, and H. Pitsch, Phys. Fluids **21**, 055102 (2009).
10 C. M. Kaul, and V. Raman, Phys. Fluids **23**, 035102 (2011).
11 C. D. Pierce, and P. Moin, Phys. Fluids **10**, 3041 (1998).
12 S. S. Girimaji, and Y. Zhou, Phys. Fluids **8**, 1224 (1996).
13 D. Veynante, and R. Knikker, J. Turbul. **7**, N35 (2006).
14 A. W. Cook, J. J. Riley, and G. Kosály, Combust. Flame **109**, 332 (1997).
15 M. Ihme, and Y. C. See, Combust. Flame **157**, 1850 (2010).
16 M. Ihme, J. Zhang, G. He, and B. Dally, Flow Turbul. Combust **89**, 449 (2012).
17 M. Ihme, and H. Pitsch, Combust. Flame **155**, 90 (2008).
18 Y. Chen, and M. Ihme, Combust. Flame **160**, 2896 (2013).
19 Y. C. See, and M. Ihme, Proc. Combust. Instit. **35**, 1225 (2015).
20 L. Wang, Combust. Flame **175**, 259 (2017).
21 A. G. Class, B. J. Matkowsky, and A. Y. Klimenko, J. Fluid Mech. **491**, 11 (2003).
22 B. B. Dally, A. R. Masri, R. S. Barlow, and G. J. Fiechtner, Combust. Flame **114**, 119 (1998).
23 A. Kempf, R. P. Lindstedt, and J. Janicka, Combust. Flame **144**, 170 (2006).
24 T. Yang, and J. Zhang, in *Proceedings of the ASME Power conference Joint with ICOPE-17* (ASME, Charlotte, 2017).
25 W. P. Jones, and R. P. Lindstedt, Combust. Flame **73**, 233 (1988).
26 L. Wang, Z. Liu, S. Chen, and C. Zheng, Combust. Sci. Tech. **184**, 259 (2012).
27 J. P. Kim, U. Schnell, and G. Scheffknecht, Combust. Sci. Tech. **180**, 565 (2008).
28 Y. Guo, *Filtered Turbulent Flamelet Model for Turbulent Combustion Simulation*, Dissertation for Master's Degree (Shanghai Jiao Tong University, Shanghai, 2019), pp. 25-34.